<u>Book Chapter</u>

Optical Pattern Recognition via a Translation Sensitivity Adjustable Compact Optical Correlator

Hua-Kuang Liu and Yahong Jin
University of South Alabama
Mobile, Alabama 36688-0002
Neville Marzwell
NASA - Jet Propulsion Laboratory
California Institute of Technology
Pasadena, California 91109-8099
Luzhong Cai
Shangtung University
Gilan, Shangtung, China

A translation sensitivity adjustable compact optical correlator (TSACOC) utilizing a convergent reference wave has been designed and tested. Its properties and performances, including the location of the correlation peak and the effects of lateral and longitudinal displacements for both filters and input images, are systematically analyzed based on the nonparaxial approximation for the reference beam. The theoretical analyses have been verified in experiments. By discussing the practical problems encountered, we have found that the tolerance of the system to the input lateral displacement can be conveniently increased by changing a geometric factor of the system. This property is very important to a TSACOC with a pinhole aperture attached to an ordinary detector at a fixed place. In addition, the effectiveness of the TSACOC for fingerprint recognition is also presented.

Keywords: correlation; correlator; pattern recognition; translation sensitivity; correlation degradation; nonparaxial diffraction; fingerprint identification.

1   Introduction

Since the advent of the Vander Lugt technique for the synthesis of an optical matched spatial filter (MSF)[1], there have been many demonstrations of this pattern recognition method on diverse classes of input data. Owing to the quasi-periodic structures (of the ridges and valleys) of the fingerprints, it seems natural to examine these patterns in the frequency domain. In fact, several schemes for this purpose have been proposed and experimentally verified in the past. These include Vander Lugt correlators[2,3], joint transform correlators[4,5], and an optical Fourier transform with a ring-wedge detector[6,7]. Generally an all-optical Vander Lugt correlator is simpler and less expensive in comparison with the hybrid system using a computer and a spatial light modulator (SLM), and is thus more desirable for an economic pattern recognition system with moderate accuracy.

The basic Vander Lugt correlators have usually been divided into two categories: the classical 4f system and the scaling correlator[8]. In the latter the distance between the object plane and the filter plane may be changed to match the wavelength difference in recording and reconstruction. In order to understand the practical performance of a correlator, the effects of different factors on correlation degradation have been investigated[9,10].

In practice there are two important requirements for a portable low-cost correlator, namely, the compactness of the reconstruction system and the repeatability of the correlation results. To meet the first requirement, we adopt an optical architecture in which a convergent reference beam instead of a plane wave is used to fabricate the MSF, so that no lens is needed behind the MSF plane in the process of correlation. This system is here referred to as the translation sensitivity adjustable compact optical correlator (TSACOC). This paper is aimed at a systematically analysis for the TSACOC system from the viewpoints of both theory and practice. For example, the influence of filter displacement was previously investigated[9,10]. In practice, however, the position of the filter can be precisely calibrated and then fixed before it is used for recognition. The repositioning error more likely to happen is the displacement of the input images (e.g. the fingerprints) at different times during addressing process, which will affect the apparent correlation intensity received by a detector at a fixed place. Therefore it is necessary to know the exact location of the correlation peak and its movement due to the input displacement. The analyses we provided here include complete calculations of the coordinates of the correlation spot and the effects of small displacements for both of the filter and the object. In addition, we have derived a simple method to reduce the sensitivity of the object displacement on the detected correlation intensity, and it has been verified by our experimental results.

In the TSACOC system, since the focal point of the reference beam is usually not far enough from the filter plane, we adopted the more accurate nonparaxial representations of a spherical wave and its diffraction field for the reference beam in the detailed theoretical investigation of the TSACOC system. In the following sections, the experimental results will be presented and the conclusions will be derived.

2   Theoretical Analyses of the TSACOC System

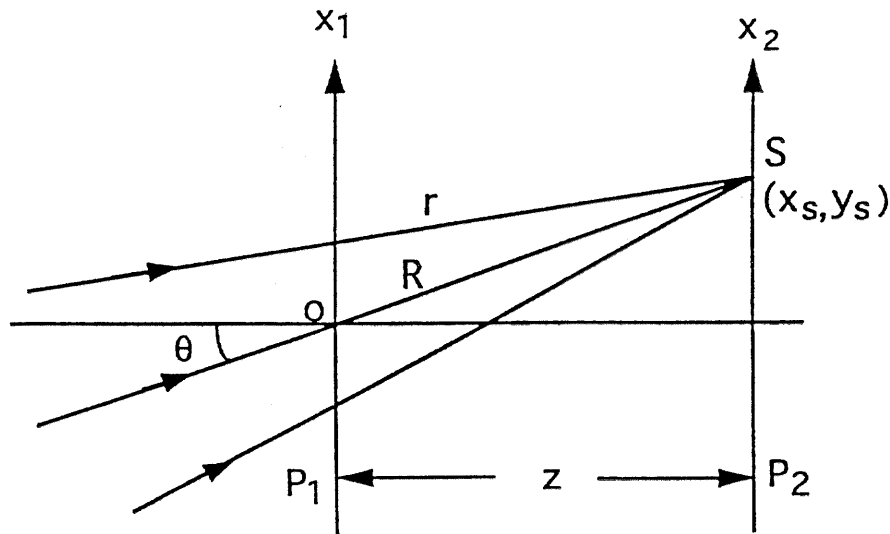### 2.1   Nonparaxial Approximations of an Oblique Spherical Wave and Its Diffraction Field

Figure 1 Schematic representation of a nonparaxial convergence wave.

In Fig.1 we show a convergent wave passing through plane P_1 and focusing at a certain point $S(x_s, y_s)$ in plane P_2. According to the paraxial approximation[11], the distance from an arbitrary point (x_1, y_1) in P_1 to point S should be

$$r = \sqrt{z^2 + (x_1 - x_s)^2 + (y_1 - y_s)^2} = z + \frac{(x_1 - x_s)^2 + (y_1 - y_s)^2}{2z} + \cdots \tag{1}$$

where z is the distance between the two parallel planes P_1 and P_2. If

$$(x_1 - x_s)^2 + (y_1 - y_s)^2 \ll z^2, \tag{2}$$

we may take into account only the first two terms in Eq.(2) and neglect others. However, when the oblique angle θ is not very small (e.g., >15°), the condition above may not be satisfied. In this case we can use the following nonparaxial representation,

$$r = \sqrt{R^2 + x_1^2 + y_1^2 - 2x_1 x_s - 2y_1 y_s} = R + \frac{x_1^2 + y_1^2 - 2x_1 x_s - 2y_1 y_s}{2R} + \cdots, \tag{3}$$

where R=OS. The similar requirement to keep only the first two terms in Eq.(3) is

$$\left| x_1^2 + y_1^2 - 2x_1 x_s - 2y_1 y_s \right|^2 \ll R^2, \tag{4}$$

which is much less stringent than Eq.(2).

Based on this nonparaxial approximation, the light distribution at plane P_1 can be expressed as

$$u(x_1, y_1) = \exp\left[\frac{i\pi}{\lambda R} \left(x_1^2 + y_1^2 - 2x_1 x_s - 2y_1 y_s \right) \right], \tag{5}$$

where all constants independent of x_1 and y_1 are and will be ignored throughout this paper without loss of any physical meaning.

Employing the Fresnel diffraction theory[11], we can derive the light field distribution in plane P_2 when a convergent wave passes through a mask at plane P_1 with a complex amplitude transmittance $t(x_1, y_1)$ as

$$u(x_2, y_2) = \iint t(x_1, y_1) \exp\left\{ -i\frac{2\pi}{\lambda R} \left[(x_2 - x_s)x_1 + (y_2 - y_s)y_1 \right] \right\} dx_1 dy_1, \tag{6}$$

which is simply a Fourier transform of $t(x_1, y_1)$ with a certain scale relation between the space and frequency domains.

2.2 Basic Recording and Reconstruction Processes and the Location of the Correlation Peak
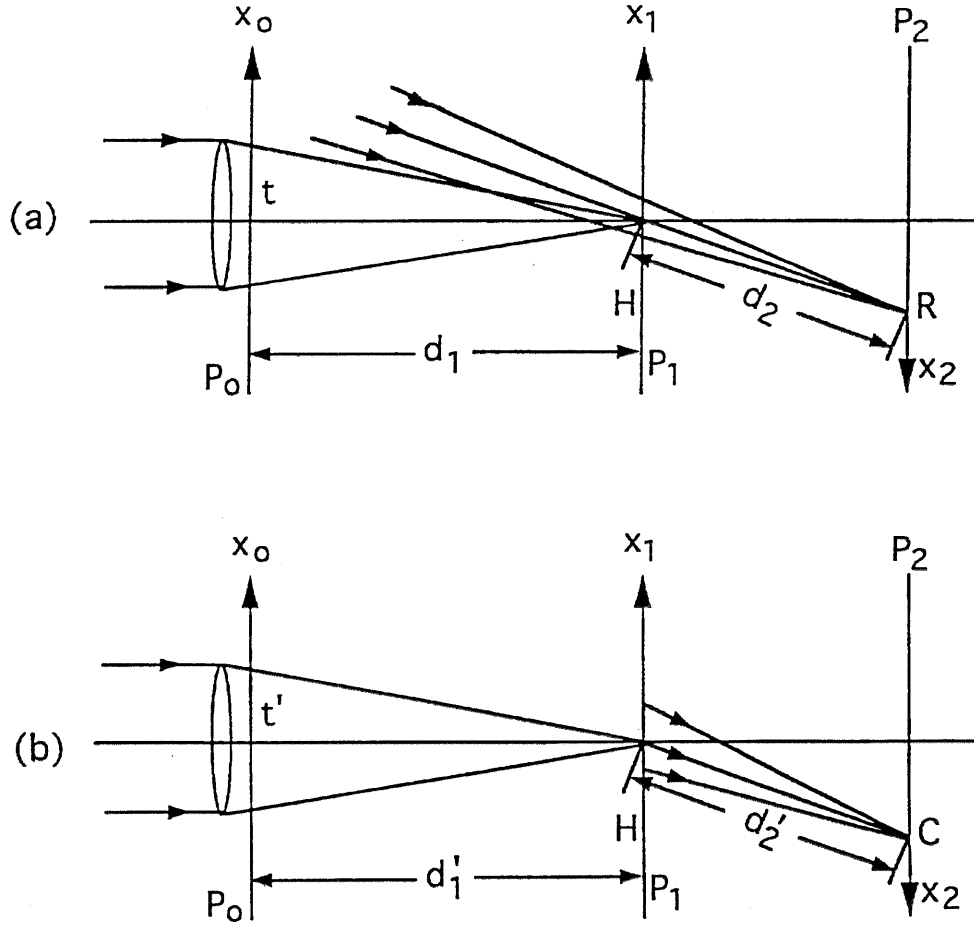
Figure 2 Basic geometry of the TSACOC: (a) recording and (b) reconstruction

The basic recording and reconstruction processes for a TSACOC are shown in Fig.2(a) and (b), where P_0, P_1 and P_2 denote the object plane, the MSF plane and the correlation plane, respectively. For the sake of generality, the parameters for the wavelengths and geometry in recording (λ, d_1, d_2) and reconstruction (λ', d_1', d_2') are assumed to be different. Noticing that the positive directions of axes (x_2, y_2) have been reversed compared with (x_0,y_0) and (x_1,y_1), we may write the light fields of the object wave and the reference wave in plane P_1 as

$$u_o(x_1,y_1) = T\left(\frac{x_1}{\lambda d_1}, \frac{y_1}{\lambda d_1}\right)\exp\left[\frac{i\pi}{\lambda d_1}\left(x_1^2 + y_1^2\right)\right], \tag{7}$$

$$u_r(x_1,y_1) = \exp\left[-\frac{i\pi}{\lambda d_2}\left(x_1^2 + y_1^2 + 2x_r x_1\right)\right], \tag{8}$$

respectively, here we assume that the reference beam converges upon a point $R(x_r,0)$ in plane P2, and T is the Fourier transform of the input function t.

In the reading process, the input image with amplitude $t'(x_0,y_0)$ is supposed to be displaced by the distances a and b in the x and y directions respectively, thus the input function become $t'(x_0-a,y_0-b)$, and the object wave field at plane P1 is

$$u_o'(x_1,y_1) = T\left(\frac{x_1}{\lambda' d_1'},\frac{y_1}{\lambda' d_1'}\right)\exp\left[\frac{i\pi}{\lambda' d_1'}(x_1^2 + y_1^2)\right]\exp\left[-i\frac{2\pi}{\lambda' d_1'}(ax_1 + by_1)\right].\tag{9}$$

The effective term of the light distribution just behind the filter H at plane P1 in the reconstruction process is

$$u_1(x_1,y_1) = u_o'u_o^*u_r = T\left(\frac{x_1}{\lambda' d_1'},\frac{y_1}{\lambda' d_1'}\right)T^*\left(\frac{x}{\lambda d_1},\frac{y}{\lambda d_1}\right)$$

$$\times\exp\left\{-i\frac{\pi}{\lambda d_2}\left[\left(1+\frac{d_2}{d_1}-\frac{\lambda d_2}{\lambda' d_1'}\right)(x_1^2 + y_1^2) + 2x_r x_1 + 2\frac{\lambda d_2}{\lambda' d_1'}(ax_1 + by_1)\right]\right\}.\tag{10}$$

Comparing the exponential term in this equation with the nonparaxial expression of a convergent wave, we find that the location of the correlation peak (i.e. the focal point, C, of the beam diffracted by the filter) is determined by the following equations,

$$x_c = \left[1-(1-\gamma)\frac{d_2}{d_1}\right]\left(x_r + \frac{d_2}{d_1}\gamma a\right),$$

$$y_c = \left[1-(1-\gamma)\frac{d_2}{d_1}\right]\frac{d_2}{d_1}\gamma b,\tag{11}$$

$$d_2' = \left[1-(1-\gamma)\frac{d_2}{d_1}\right]\frac{\lambda}{\lambda'}d_2,$$

where $\gamma=\lambda d_1/\lambda' d_1'$ is the matching factor. And the light distribution at plane P2 should be the inverse Fourier transform of Eq.(10), i.e.,

$$u_2(x_2,y_2) = \iint u_1(x_1,y_1)\exp\left\{i\frac{2\pi}{\lambda' d_2'}[(x_2 - x_c)x_1 + (y_2 - y_c)y_1]\right\}dx_1 dy_1$$

$$= \left[t'\left(\frac{d_1'}{d_2'}x_2,\frac{d_1'}{d_2'}y_2\right)\otimes t\left(\frac{\lambda d_1}{\lambda' d_2'}x_2,\frac{\lambda d_1}{\lambda' d_2'}y_2\right)\right]*\delta(x_2 - x_c,y_2 - y_c),\tag{12}$$

where $\otimes$ and $*$ denote the correlation and convolution respectively.

For the case of a complete matching, $\gamma=1$, Eqs.(11) and (12) can be simplified as

$$x_c = x_r + \frac{d_2}{d_1} a,$$

$$y_c = \frac{d_2}{d_1} b, \tag{13}$$

$$d_2' = \frac{\lambda}{\lambda'} d_2.$$

$$u_2(x_2, y_2) = \left[t'\left(\frac{d_1}{d_2} x_2, \frac{d_1}{d_2} y_2 \right) \otimes t\left(\frac{d_1}{d_2} x_2, \frac{d_1}{d_2} y_2 \right) \right] * \delta(x_2 - x_c, y_2 - y_c). \tag{14}$$

2.3   Lateral Displacement of Filters

In this case we assume $\gamma=1$, t' and t are located at the same position, but in the reconstruction step the filter H is displaced slightly, i.e., α in x direction and β in y direction. Referring to Eqs.(7) and (8), and replacing x_1 and y_1 by $x_1-\alpha$ and $y_1-\beta$ in the product $u_0' u_0^*$, we obtain the light distribution just behind H,

$$\begin{aligned}
u_1'(x_1, y_1) &= u_0' u_0^* u_r \\
&= T\left(\frac{x_1}{\lambda d_1}, \frac{y_1}{\lambda d_1} \right) T^*\left(\frac{x_1 - \alpha}{\lambda d_1}, \frac{y_1 - \beta}{\lambda d_1} \right) \exp\left[-i \frac{\pi}{\lambda d_2}\left(x_1^2 + y_1^2 + 2x_c' x_1 + 2y_c' y_1 \right) \right],
\end{aligned} \tag{15}$$

where

$$x_c' = x_r - \left(1 + \frac{d_2}{d_1} \right)\alpha,$$

$$y_c' = -\left(1 + \frac{d_2}{d_1} \right)\beta \tag{16}$$

are the coordinates of the correlation peak. And the light field at plane P2 is

$$\begin{aligned}
u_2'(x_2, y_2) &= \left\{ t'\left(\frac{d_1}{d_2} x_2, \frac{d_1}{d_2} y_2 \right) \otimes \left[t\left(\frac{d_1}{d_2} x_2, \frac{d_1}{d_2} y_2 \right) \exp\left(i \frac{2\pi}{\lambda d_2}(\alpha x_2 + \beta y_2) \right) \right] \right\} \\
&\quad * \delta(x_2 - x_c', y_2 - y_c').
\end{aligned} \tag{17}$$

Assuming t'=t, we obtain the intensity at the center of the auto-correlation distribution as

$$I_c = \left| \iint \left| t\left(\frac{d_1}{d_2} x, \frac{d_1}{d_2} y \right) \right|^2 \exp\left(i \frac{2\pi}{\lambda d_2}(\alpha x + \beta y) \right) dx dy \right|^2. \tag{18}$$

By introducing the performance P of the system as the signal-to-noise ratio, SNR, based on the intensity distribution at the output plane as defined by Vander Lugt[9], and limiting our treatment to the case that the noise spectral density is uniform, we can derive the normalized performance of the system as

$$P = \frac{\left| \iint \left| t\left(\frac{d_1}{d_2}x, \frac{d_1}{d_2}y \right) \right|^2 \exp\left[i\frac{2\pi}{\lambda d_2}(\alpha x + \beta y) \right] dxdy \right|^2}{\left| \iint \left| t\left(\frac{d_1}{d_2}x, \frac{d_1}{d_2}y \right) \right|^2 dxdy \right|^2}. \tag{19}$$

When the inputs are the images of fingerprints, we may use the following binary function shown in Fig.3 to simulate their periodic structure in one dimension,

$$t(x) = \sum_{n=-N/2+1}^{N/2} rect\left(\frac{x-(2n-1)a}{a} \right), \tag{20}$$

where d=2a is the period of the pattern. Substituting this expression into Eq.(19), we yield

$$P = \frac{\sin c^2\left(\frac{d\alpha}{2\lambda d_1} \right) \sin^2\left(\frac{N\pi\alpha d}{\lambda d_1} \right)}{N^2 \sin^2\left(\frac{\pi\alpha d}{\lambda d_1} \right)}. \tag{21}$$

For a small α and N>>1, this equation can be reduced to

$$P = \sin c^2\left(\frac{\alpha L}{\lambda d_1} \right) \tag{22}$$

where L=Nd is the width of the input image. This result is similar to that obtained by Vander Lugt for the input of a single rect(x) function[9]. But now with a periodic function we may further conclude that the performance P is independent of the parameters d_2, N and d themselves, and related only to d_1 and the total width of the image, L.
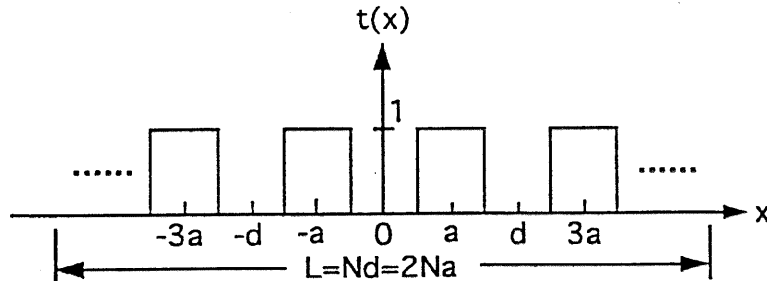

Figure 3 Simplified model of fingerprints in one dimension: Ronchi grating

Eq.(22) indicates that the maximum lateral displacement of a filter, corresponding to the first null of P, is $\alpha_M = \lambda d_1/L$. The physical meaning of this result can be explained by the diffraction theory. In the recording step the size of the diffraction spot at the filter plane is approximately α_M. If the filter is shifted by α_M, the position of the same spot in the step of reconstruction will be entirely separated from its original recording position, and hence the correlation peak will disappear.

2.4 Longitudinal Displacement of Filters

Vander Lugt discussed the effect of the longitudinal displacement of the filters on the correlation output when the input object is located off-axis[9]. We present here an analysis for the case that the object is centered on the axis. In Fig.4 the MSF is displaced a distance δ longitudinally from the recording plane P_1 to a new plane P_2. Obviously the spot A in H, corresponding to a specific spatial frequency $f_x = x_A/\lambda d_1$, is shifted and becomes the point B in H'. The distance shifted is
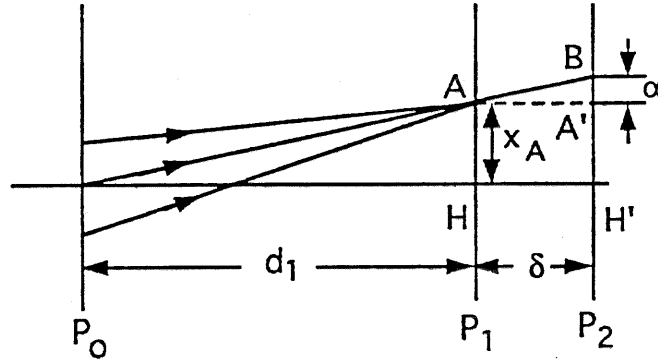

Figure 4 Effect of the MSF longitudinal displacement

$$\alpha = \frac{x_A \delta}{d_1} = \lambda f_x \delta = \frac{\lambda \delta}{d} \tag{23}$$

where $d=1/f_x$ is the corresponding period of f_x. By substituting Eq.(23) into Eq.(22), we have

$$P = \operatorname{sinc}^2\left(\frac{N\delta}{d_1}\right) \tag{24}$$

where $N=L/d$ which stands for the spatial bandwidth (SBW) of the input image if we simply treat it as a 1-D grating. In the 1-D case, the maximum displacement is $\delta_M = d_1/N$, which is inversely proportional to N, as illustrated in Fig.5.
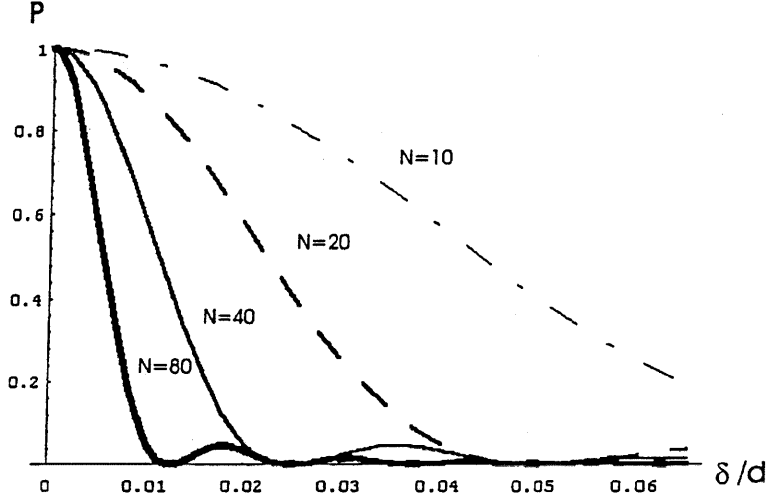
Figure 5 Dependence of the performance of a TSACOC on the MSF longitudinal
displacement and the SBW of the input images.

By combining Eq.(23) and the corresponding result obtained by Vander Lugt[9], a
general expression of the effective mismatched displacement, arising from the longitudinal
mispositioning of the MSF and applicable for both of the axial and non-axial input images,
may be written as

$$\alpha = \left(\frac{\lambda}{d} + \frac{x_o}{d_1} \right) \delta \tag{25}$$

where x_0 is the distance from the center of input image to the optical axis of the system.
Usually $\lambda \ll d$, $x_0 \ll d_1$, so that $\alpha \ll \delta$, which means that the influence of the longitudinal
displacement of filters is much less than that of the lateral one.

2.5   Lateral displacement of Objects

Now we consider the case that the filter is positioned precisely at its original location, and
$\lambda' = \lambda$, so $d_1' = d_1$ and $\gamma = 1$ in Fig.2, but the center of the object is displaced from (0,0) to
(a,b). The result of Eq.(12) implies that this displacement has no effect on the intensity of
the correlation peak. Thus the displacement does not affect the performance of the system
as can be seen from Eq.(19) (P=1 when $\alpha = \beta = 0$). This is the shift invariance property of
the MSF. But the location of the correlation peak is changed as indicated by Eq.(13).

2.6   Longitudinal Displacement of Objects

If every condition in the reconstruction step remains the same as that in the recording step,
but the input object just makes a small longitudinal displacement (i.e., $d_1' \neq d_1$), then by

letting $\lambda' = \lambda$ and a=b=0 in Eq.(11), we can derive the resultant position of the correlation
peak,

$$x_c' = \left(1 - \frac{d_2}{d_1}\Delta\right)x_r,$$

$$y_c' = 0,$$

$$d_2' = \left(1 - \frac{d_2}{d_1}\Delta\right)d_2, \tag{26}$$

where $\Delta = (d_1' - d_1)/d_1$, defined as the relative variation of d_1, is assumed to be much less than 1. Clearly the relative variations of x_c' and d_2' are both equivalent to $(-d_2/d_1)\Delta$.

On the other hand, according to Eq.(12), the central intensity of the correlation peak now becomes

$$I_c'(\Delta) = \iint \left| t'\left(\frac{d_1'}{d_2'}x, \frac{d_1'}{d_2'}y\right)t\left(\frac{d_1}{d_2}x, \frac{d_1}{d_2}y\right)\right| dxdy. \tag{27}$$

For $t'=t$, this intensity corresponds to the maximum correlation between two images with the same pattern but a scale variation factor $m = d_1'/d_1 = (1+\Delta)$. Generally a greater Δ yields a smaller I_c'. The concrete expression of I_c' depends on the specific structure of the input image. Again we use the Ronchi grating model here to simplify the fingerprint in the one dimensional case to obtain the normalized central intensity of the correlation peak. After some calculation under the conditions $|\Delta|<<1$ and $N|\Delta|<1/2$, we have

$$i_c = \frac{I_c'(\Delta)}{I_c'(\Delta=0)} = \left(1 - N|\Delta|\right)^2 \tag{28}$$

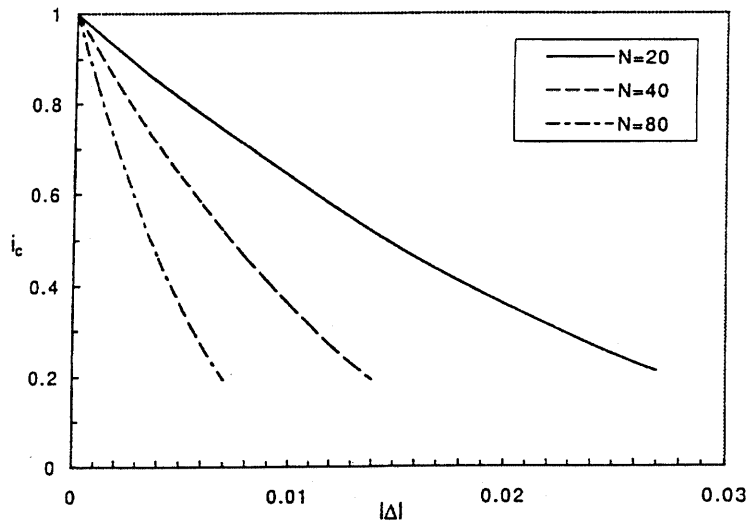where N is still the SBW of the input grating.

Figure 6 Dependence of the normalized central intensity of the correlation peak on the object longitudinal displacement and the SBW of the input images.

The dependence of i_c upon Δ and N is shown in Fig.6. Evidently i_c decreases more rapidly with a greater N.

2.7   Effect of the Out-of-focus Error of MSF Positioning

The shift invariance property is held true only if the MSF is exactly located at the focal plane of the object beam. Practically the longitudinal positioning of MSF may have a small error ε as shown in Fig.7, where P$_1$ is the focal plane, and P$_1$' is the plane where the MSF is positioned in both the recording and reconstruction processes. If the object has a small lateral displacement, a, between the two processes, the spatial frequency spectra in H will be mismatched. Strictly the mismatching quantities slightly vary for different frequencies, but the average value may be written as $\alpha = a\varepsilon/d_1$ with reference to Fig.7. By substituting this value into Eq.(22), we obtain the performance of the system,

$$P = \operatorname{sinc}^2\left(\frac{La\varepsilon}{\lambda d_1^2}\right) \tag{29}$$

and the maximum allowable displacement of an object corresponding to the first zero of P is thus

$$a_M = \frac{\lambda d_1^2}{L\varepsilon} = \frac{d_1}{\varepsilon}\alpha_M \tag{30}$$

which is much larger for a small ε than the maximum lateral displacement of the filters, α_M, given in section 2.3.
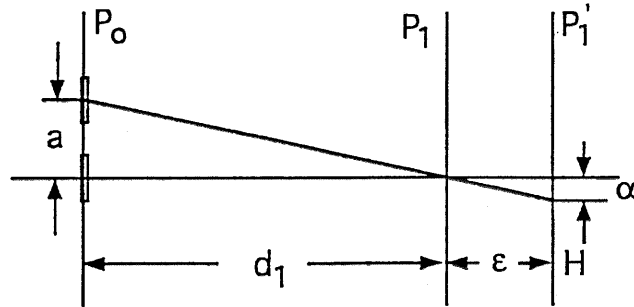

Figure 7 Effect of the out-of-focus error on the MSF positioning

3   Practical Considerations and Experimental Results

3.1   Some Practical Considerations Based on the Theoretical Analyses

The theoretical results obtained above can be briefly summarized as follows:

(1) The filter displacement affects both the position and the intensity of the correlation peak, and the influence of the longitudinal displacement is much less than that of the lateral displacement. The degradation of the correlation signal arising from the displacements is more serious for an input image with a greater SBW.

11

(2) While the lateral displacement of objects affects the position of the correlation peak instead of its intensity, the longitudinal displacement changes both of them, and the decline of the peak intensity also depends upon the SBW of the input image.

(3) The MSF plane should be placed exactly at the focal plane of the object wave to realize the lateral shift invariance of the system, but this requirement for the longitudinal positioning accuracy is not very critical compared with the MSF lateral displacement.

For a practical product of the TSACOC, we may make some efforts to improve its performance. The problem of MSF positioning is relatively easy to solve, since we can precisely determine the location of the focal plane , place the MSF at this fixed plane before recording, and then carefully replace the MSF in the reconstruction process to its initial place by means of detecting the maximum peak intensity when the MSF is moving laterally. The longitudinal positioning accuracy of the input images can also be satisfied if we input the images each time at a fixed plane.

The reposition error of the objects, on the other hand, may be an unavoidable problem for a real input. This is because the finger positions may be slightly different from time to time. The rotation variation may be controlled by using a confining box, however, the translation displacement is inevitable as people may press their fingers with varyingt pressures, which in turn will vary the correlation peak position.

In order to reduce the space and cost of a TSACOC, a small area detector, instead of a detector array, with the use of a small pinhole as a receiving aperture, is preferable. The size of the pinhole should be large enough to detect the correlation peak and tolerate a certain amount of input displacement, and small enough to reject most of the background noise. For example, if we consider the fingerprint as an one dimensional grating with a, fundamental spatial frequency of 2 line pairs/mm, the width of its correlation peak is approximately 0.5mm for the case $d_2/d_1 = 1$, and we may choose the diameter of the pinhole around 1mm.

As mentioned above, the correlation peak will move laterally with a laterally shifted input image. Obviously it is not convenient to adjust the pinhole position each time to match the input displacement. However, Eqs.(11) and (13) reveal an important fact: this translation sensitivity is strongly dependent on the geometric configuration of the system, namely, the parameter d_2/d_1. In the practical case of $\gamma=1$, the variation of x_c, y_c is simply proportional to d_2/d_1. It suggests that we can reduce the translation sensitivity simply by decreasing d_2/d_1 . We will describe the experimental verification of this method in the next section, and then give the experimental results of a TSACOC for fingerprint recognition.

3.2 Experimental Verification of the Depression of the Sensitivity of Object Lateral Displacement

The basic architecture for the MSF recording is shown in Fig.2(a). To verify the dependence of the sensitivity of the object translation displacement upon d_2/d_1 , we made several filters for different d_2/d_1, and measured with these filters the variation of the correlation intensities received by a detector with a pinhole aperture of about 1.2mm diameter at a fixed place. The experimental results are shown in Fig.8, where the vertical coordinate stands for the relative intensity, the horizontal coordinate denotes the translation displacement of the input image, and the three curves correspond to $d_2/d_1=1$, 1/2 and 1/4, respectively. It is clear that the smaller the d_2/d_1 is, the wider the tolerable displacement range will be. Specifically, the widths of the three curves above the middle intensity (0.5)

are about 1.0 mm, 2.1 mm and 4.1 mm, respectively. These data fairly agree with our theoretical analysis.
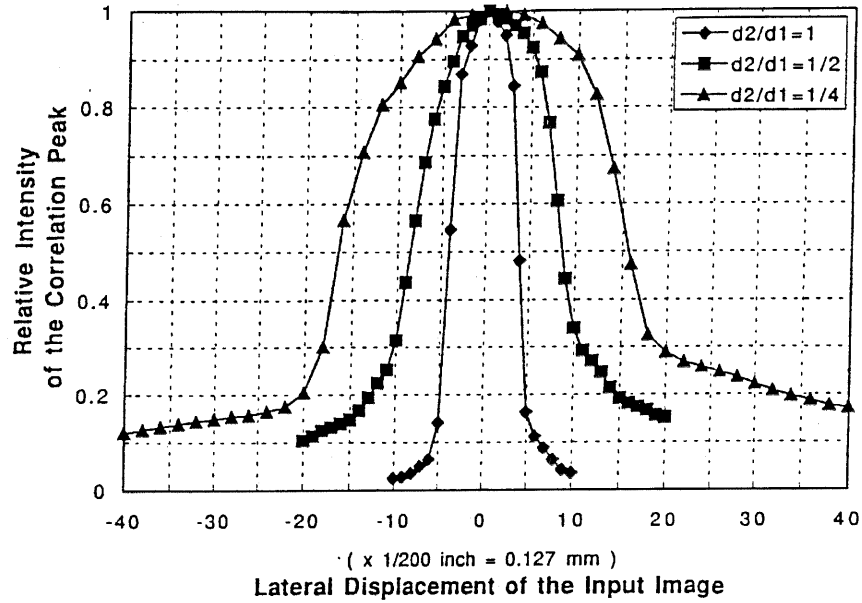

Figure 8 Experimental results verifying the effectiveness of the method of increasing the object lateral displacement tolerance by decreasing d_2/d_1

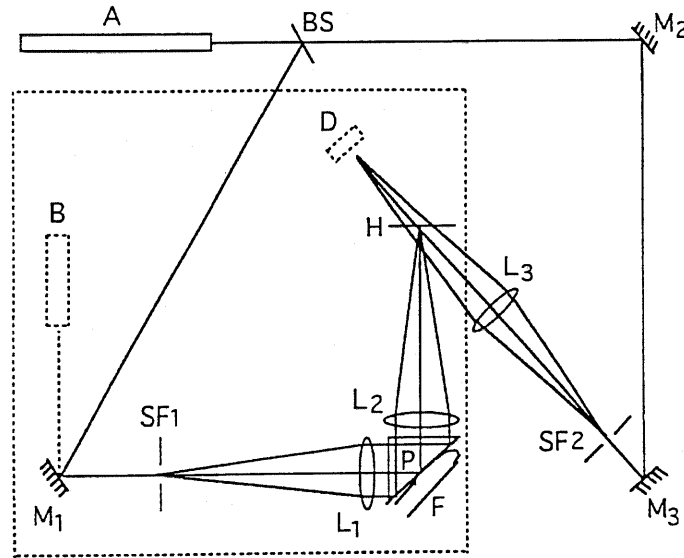## 3.3 *Experimental Setup and Results for Fingerprint Recognition*

Figure 9 Experimental set-up of a TSACOC

Our experimental setup of a TSACOC for fingerprint recognition is shown in Fig.9, where all the elements drawn with solid lines are used for recording the MSF, A is a He-Ne laser, BS stands for the beam splitter, M-mirror, SF-spatial filter, L-lens, H-MSF, P-prism, and F-finger. This system utilizes a 90-deg prism to realize the real time input of the fingerprints via total internal reflection mechanism[12]. The focal length of L_1 and L_2 is 40

13

cm, and the distance between the center of H and the focal point of the reference beam is about 14 cm, so $d_2/d_1 = 0.35$. To ensure the repositioning accuracy of the finger each time, we use a blocking device to confine the position of finger.
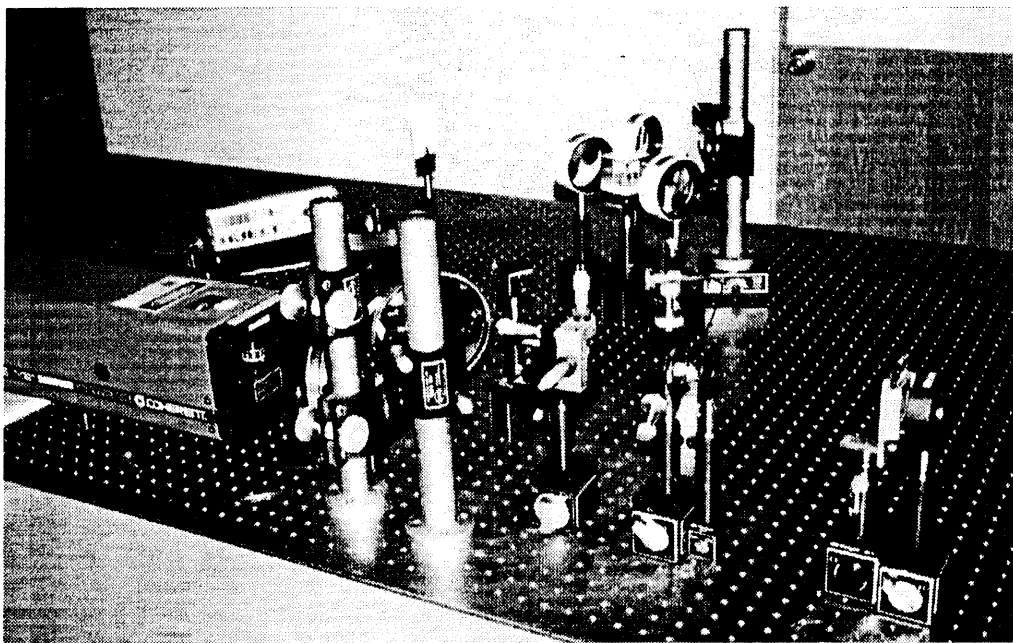

Figure 10 A photograph showing the hardware arrangement for the experiment

The laboratory bench hardware arrangement of the system are represented in Figures 10 and 11. In Fig. 10, an argon ion laser is shown in the lower left hand corner is used to illuminate the optical system. Beam splitters and spatial filters are also shown. Fig. 11 shows a view of the system from the other side of the optical bench. A power showing the measured laser power is shown in the fireground. Blue laser beam is clearly visible in the picture.
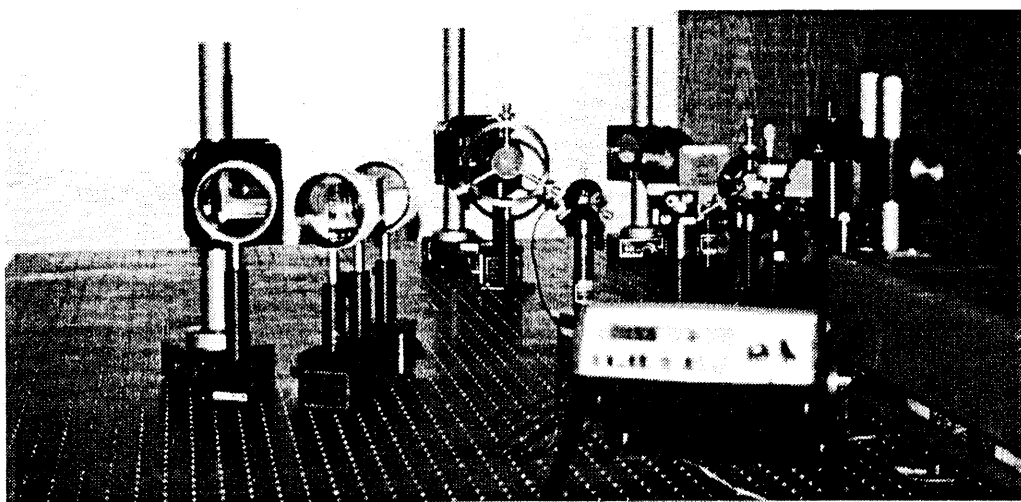

Figure 11 A photograph showing the same experimental setup as viewed from a different perspective with laser light and photometer during measurement

Another problem affecting the final correlation results is the zero spatial frequency (DC) term of the object beam, whose relative value is 0.5 for the Ronchi grating model, or even greater than 0.5 in the practical prism input case. The correlation between DC terms of two different images may introduce significant background peak intensity. A simple approach to eliminate this effect is to overexpose the MSF in the recording step, so that the DC portion at the center of the spectrum becomes entirely dark and hence has no diffraction function.

A MSF can be replaced to its original position through moving the filter continuously and observing the correlation peak intensity received by a detector with a pinhole centered at the focal point of the reference beam until the intensity reaches its maximum. We suggest "trial and error" in searching for the right way of replacing the user's finger.

In Fig.12 we give a statistical result of our experiments, where the height of each post represents the detected relative intensity, A, B and C are for auto-correlation (averaged over 16 times), across-correlation (10 times) and DC input only (no image, 20 times), respectively. If we set an appropriate threshold, 0.6 for instance, we can realize the fingerprint recognition.
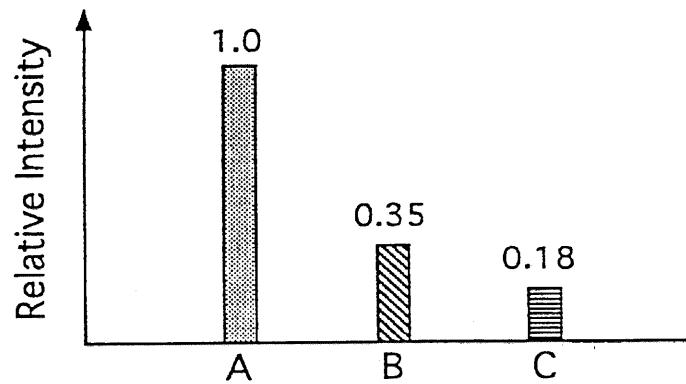

Figure 12 A statistical experiemental result of the TSACOC for fingerprint recognition

As a real correlator product for identification, we need only to use the part within the dashed line square of Fig.9, where A is a small He-Ne laser.

4. Optical Pattern Recognition Application

The application of the TSACOC is not limited to finger print recognition. A diagram illustrating another application of the TSACOC is presented in Fig. 13 as shown below.
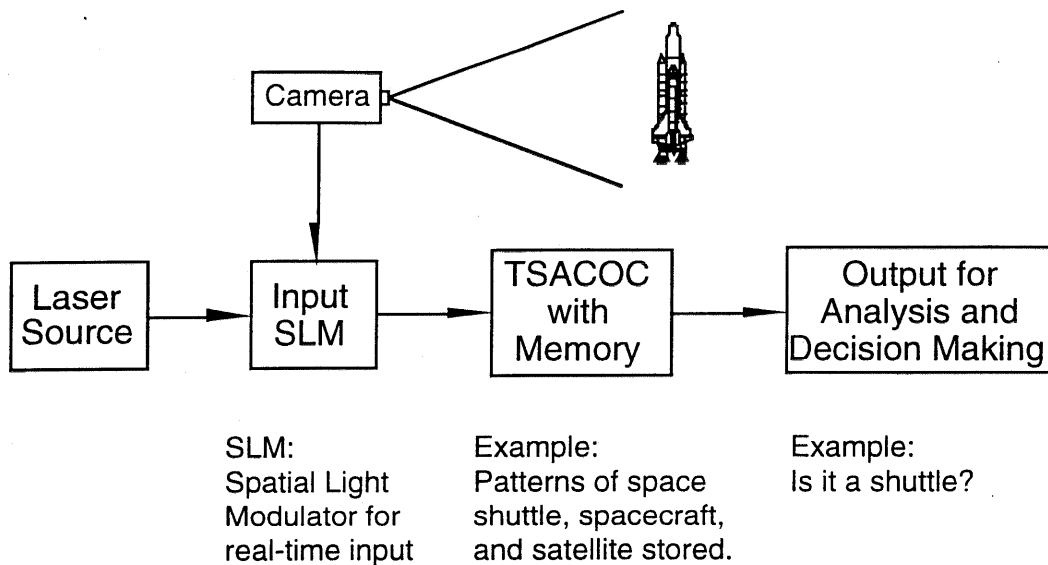
Figure 13. A block diagram illustrating a representative application of the innovative TSACOC.

Assuming that a compact TSACOC is equipped on a space vehicle and looking for another space object such as a space shuttle for docking and rendezvous. The patterns of known objects have been stored in the TSACOC. A CCD video camera is used to look at the targets. The output of the camera is applied to the electronically addressed spatial light modulator(SLM) which is illuminated by a laser source. The laser illuminated image pattern is applied to the TSACOC and compared with the image stored in the holographic memory of the TSACOC. The output is used for analyses and automatically making decisions to determine whether the shuttle or other objects are found.

5.   Conclusions

We have designed, analyzed and tested a TSACOC and applied it for pattern recognition. We have systematically examined its properties, including the location of the correlation peak, the effects of filter displacement, object displacement, and the out-of-focus positioning of the MSF plane. Based on the theoretical study, we find a simple way to reduce the sensitivity of a TSACOC to the input lateral displacement, which is the error most likely to happen for a real time input system, by reducing the ratio d_2/d_1. This ability adds an important advantage of the TSACOC, the relatively large tolerance of the input positioning deviation, to its simplicity and compactness. The experimental results we obtained have verified the expectations of our analyses and proved the effectiveness of the TSACOC for fingerprint identification.

Acknowledgment

References

1. A. B. Vander Lugt, "Signal detection by complex spatial filtering," *IEEE Trans. Inf. Theory* **IT-10,** 139-145 (1964).
2. V. V. Horvath, J. M. Holeman and C. Q. Lemmond, "Holographic technique recognizes fingerprints," *Laser Focus* **6**, 18-23 (1967).
3. F. T. Gambe, L. M. Frye, and D. R. Grieser, "Real-time fingerprint verification system," *Appl. Opt.* **31**, 652-655 (1992).
4. C. S. Weaver and J. W. Goodman, "A technique for optically convolving two functions," *Appl. Opt.* **5**, 1248 (1966).
5. K. H. Fielding, J. L. Horner and C. K. Makekau, "Optical fingerprint identification by binary joint transform correlation," *Opt. Eng.* **30**(12), 1958-1961 (1991).
6. J. Ohta, J. Sharpe, and K. Johnson, "An optoelectronic smart detector array for the classification of fingerprints," *Opt. Commun.* **111**, 451-458 (1994).
7. Zikuan Chen, Ying Sun, Yanxin Zhang, and Guoguang Mu, "Hybrid optical/digital access control using fingerprint identification," *Opt. Eng.* **34**(3), 834--839 (1995).
8. A. Vander Lugt, "Practical considerations for the use of spatial carrier-frequency filters," *Appl . Opt.* **5**(11), 1760-1765 (1966).
9. A. Vander Lugt, "The effects of small displacements of spatial filters," *Appl. Opt.* **6**(7), 1221-1225 (1967).
10. D. Casasent and A. Farman, "Sources of correlation degradation," *Appl. Opt.* **16**(6), 1652-1661 (1977).
11. J. W. Goodman, *Introduction to Fourier Optics,* McGraw-Hill, New York (1968).
12. A. Shimizu and M. Hase, "Entry method of fingerprint image using prism," *Trans. Inst. Electronic Comm. Engineers Japan*, Part D, **J67D**(5), 627 (1984).

Figure Captions

Fig.1   Schematic representation of a nonparaxial convergent wave.

Fig.2   Basic geometry of the TSACOC: (a) recording and (b) reconstruction.

Fig.3   Simplified model of fingerprints in one dimension: Ronchi grating.

Fig.4   Effect of the MSF longitudinal displacement.

Fig.5   Dependence of the performance of a TSACOC on the MSF longitudinal displacement and the SBW of the input images.

Fig.6   Dependence of the normalized central intensity of the correlation peak on the object longitudinal displacement and the SBW of the input images.

Fig.7   Effect of the out-of-focus error of the MSF positioning.

Fig.8   Experimental results verifying the effectiveness of the method of increasing the object lateral displacement tolerance by decreasing d_2/d_1.

Fig.9   Experimental setup of a TSACOC.

Fig.10 A statistical experimental result of the TSACOC for fingerprint recognition.

Biographies

Hua-Kuang Liu received his Ph.D. degree from Johns Hopkins University in Electrical Engineering. Dr. Liu is a Professor of Electrical and Computer Engineering at the University of South Alabama. He has been a Senior Research Engineer at the Jet Propulsion Laboratory, California Institute of Technology. Dr. Liu's research specialties include optical and optoelectronic computing, holography, optical information processing, optical display, optical neural networks, and laser optics. He has organized and chaired over 30 national and international conferences and served as referee for archival journals and reviewer for major funding agencies. In the area of new technology development, he has over 50 U. S. patents and NASA Awards and Certificates of Recognition for Technology Innovation. In addition, Dr. Liu has published more than 200 technical papers and delivered over 60 invited speeches and seminars. Dr. Liu is a Fellow of the Optical Society of America (OSA) and a Fellow of the SPIE-The International Society of Optical Engineering, and is listed in several national and international Who's Who publications.

Yahong Jin received her Ph.D. degree in Physics from Rensselaer Polytechnic Institute, Troy, New York in 1994. She is an Assistant Professor at the University of south Alabama. Dr. Jin has been serving as a visiting scientist at Jet Propulsion Laboratory, California Institute of Technology and is a senior optical scientist of Standard International, Inc. Dr. Jin has over 20 refereed publications. Her research interests include optical neural networks, pattern recognition, holographic display, ultrafast optical switching, optical communications, nonlinear optical phenomena, optical memory and data storage. Dr. Jin is a member of American Physical Society.

Neville Marzwell has a B.S. in Chemistry, an M.S. in Materials Science and dual Ph.D. degrees in Applied Physics and Economics from the California Institute of Technology, where he was a von Karman fellow. He has 22 years experience in aerospace and defense technology working for Honeywell, Aerojet Electro-systems, Rockwell International and the Jet Propulsion Laboratory. Some of his expertise is associated with research work in the areas of holography, optical recording and processing, image recognition and enhancement. He developed under Rome Air Development Center funding advanced integrated optics and optical fiber devices and concepts. He was instrumental in many advances in detector technology (Hg-Cd-Te and Pb-Sn-Te) and electro-optical materials such as PLZT and SBN. Dr. Marzwell was chairman of the International Non-Destructive Test and Evaluation Conference which had special emphasis on Automation and Robotics, sponsored by FAA, DoE and DoD in Albuquerque- New Mexico. He has published 46 papers in refereed and professional journals and served on various panels, workshop, conference and symposium committee.

Luzhong Cai received his BS degree in radioelectronics from Beijing (Peking) University and MS degree in Optics from Nankai University, China, respectively. Now he is a professor of the Optics Department, Shandong University, China, and a visiting scholar in the Department of Electrical and Computer Engineering, the University of California at Santa Barbara. His research interests cover physical optics with the emphases on the optical information processing, holography, optical pattern recognition and nonlinear optics. He is the author or co-author of four books and about 50 technical papers published in China (Mainland and Taiwan) and abroad, and the recipient of several awards for outstanding teaching and researching achievements in China.